

SPATIALLY DISCRETE FITZHUGH–NAGUMO EQUATIONS*

CHRISTOPHER E. ELMER[†] AND ERIK S. VAN VLECK[‡]

Abstract. We consider pulse and front solutions to a spatially discrete FitzHugh–Nagumo equation that contains terms to represent both depolarization and hyperpolarization of the nerve axon. We demonstrate a technique for deriving candidate solutions for the McKean nonlinearity and present and apply solvability conditions necessary for existence. Our equation contains both spatially continuous and discrete diffusion terms.

Key words. traveling fronts and pulses, discrete diffusion

AMS subject classifications. 35K57, 74N99

DOI. 10.1137/S003613990343687X

1. Introduction. By considering an electrical circuit model with a complicated nonlinear resistor, Hodgkin and Huxley (along with Katz) modeled the ionic conductances that generate the action potential of nerve fibers. To develop their model they performed voltage and space clamping experiments on the giant axon of squids, axons which were *relatively* easy to work with because of their size. The Hodgkin–Huxley equations are a four-variable model which may be reduced to a two-variable model (the FitzHugh–Nagumo (FH-N) ODE model) which preserves much of the dynamics of the Hodgkin–Huxley system by considering fast and slow variables and slaving the other variables. When considering a chain of electrical circuits, diffusion is added as a means of propagation in the spatial variable, thus obtaining the FH-N PDE model. Since the seminal work of Hodgkin, Huxley, and Katz, similar experiments have been performed on nerve axons of vertebrates and it has been discovered that, electrically, nerve fibers behave as spatially discrete periodic structures in vertebrates. This is due to the periodically spaced active channels (nodes of Ranvier) in the myelin insulation (in the coating by Schwann cells or oligodendrocytes). Thus it is not only appropriate but correct to model motor nerves in vertebrates with equations which also have a spatially discrete periodic structure, to model with nonlinear differential-difference equations (DDEs), in particular an FH-N DDE model.

Our contribution in this paper is to consider front and pulse solutions for a FitzHugh–Nagumo system with both continuous and discrete diffusion, thus allowing one to compare and contrast the dynamics generated by spatially continuous and spatially discrete models of action potential propagation. By employing a piecewise linear bistable nonlinearity we reduce the problem to a linear inhomogeneous equation, for which candidate solutions can be derived using transform methods. The candidate solutions are then shown to be consistent with our ansatz of a front or pulse solution, a necessary condition for existence. We focus on one-front and one-pulse solutions and prove their existence using two approaches: (1) we show that consistency of the

*Received by the editors October 29, 2003; accepted for publication (in revised form) October 27, 2004; published electronically April 14, 2005. This work was supported in part by NSF grants DMS-0204573, DMS-9973393, and DMS-0139824.

<http://www.siam.org/journals/siap/65-4/43687.html>

[†]Department of Mathematical Sciences, New Jersey Institute of Technology, Newark, NJ 07102 (elmer@oak.njit.edu).

[‡]Department of Mathematics, University of Kansas, Lawrence, KS 66045 (evanvleck@math.ukans.edu).

infinite interval solution may be reduced to showing consistency on a finite interval, and (2) we use the implicit function theorem, thus showing that consistency can be obtained with a perturbation argument. Once we have derived the exact solutions and verified their existence, we investigate the solution behavior as a function of the problem parameters.

Mathematical models of the electrical behavior of axons often come from postulating an equivalent electrical circuit model (leaky underwater cable theory) of the excitable axonal membrane. Consider a single nerve fiber (axon) coated with a lipid material called myelin with periodically spaced gaps (which are commonly called nodes). Assuming the axial currents are constant, the intracellular, I_i , and the extracellular, I_e , currents between two consecutive nodes are (by Ohm's law)

$$Lr_i I_{i,n} = -(v_{i,n+1} - v_{i,n}) \quad \text{and} \quad Lr_e I_{e,n} = -(v_{e,n+1} - v_{e,n}),$$

where L is the length of the myelin sheath between the nodes, r_i and r_e are the intracellular and extracellular resistances per unit length of material, and $v_{i,n}$ and $v_{e,n}$ are the intracellular and extracellular voltages in the n th node. Using Kirchoff's laws, one obtains

$$I_{i,n-1} - I_{i,n} = I_{e,n} - I_{e,n-1} = \mu p \left(C \frac{\partial v_n}{\partial t} + I_{ion,n} \right),$$

where the quantities in the parentheses are the capacitive current and the ionic current flowing through the n th node from inside to outside, $v_n = v_{i,n} - v_{e,n}$, μ is the length of each node (here they will all be assumed to be the same), p is the perimeter length of the axon (assumed to be constant), C is the capacitance, and $I_{ion,n}$ is the ionic current at each node. The total transmembrane current at a node n is thus given by

$$(1.1) \quad p \left(C \frac{\partial v_n}{\partial t} + I_{ion,n} \right) = \frac{1}{\mu L(r_e + r_i)} (v_{n+1} - v_n + v_{n-1} - v_n).$$

The change of variables $\tau = t/(CR)$ nondimensionalizes time (where R has units $\Omega \text{ cm}^2$) and (1.1) becomes

$$\frac{dv_n}{d\tau} = \rho(v_{n+1} - 2v_n + v_{n-1}) - RI_{ion,n},$$

where $\rho = R/(\mu Lp(r_i + r_e))$. We want the transmembrane ionic current at each node to possess both a sodium and a potassium component (like an actual nerve we want both a "front" and "back" to our traveling waves), thus we use the analytically simple $RI_{ion,n} = f(v_n) + w_n$, where $f(v_n)$ represents the sodium ion current component and w_n represents the potassium ion current contribution, and we add the governing equation

$$\frac{\partial w_n}{\partial t} = b(v_n - rw_n)$$

for our potassium recovery variable w_n . Note that by setting $b = 0$, one can assume that the behavior is dominated by the leading edge behavior and that recovery is so slow that it can be treated as constant.

Related to our work on the discrete FitzHugh–Nagumo equation is the work of Anderson and Sleeman [1] on the existence and stability of equilibrium solutions, the work of Binczak, Eilbeck, and Scott [9] on ephaptic coupling in systems related to

systems of discrete FitzHugh–Nagumo equations, the work of Tonnelier [38, 39, 40], the work of Carpio and Bonilla [8], as well as the enlightening books of Keener and Sneyd [28] and Scott [36]. Work on the discrete Nagumo equation includes the work of Bell and Cosner [4], Keener [26, 27], and Zinner [44, 45] on existence, stability, and propagation failure, and the work of Mallet-Paret [31, 32] establishing a Fredholm theory for linear mixed type delay equations. Other works on discrete Nagumo type equations include [3, 5, 6, 7, 11, 12, 13, 14, 19, 23, 24]. Notable work on the existence and stability on monotone traveling fronts for the Nagumo PDE include that of Aronson and Weinberger [2] and Fife and McLeod [21] and the original work of Nagumo, Arimoto, and Yoshizawa [34]. Existence and stability of fronts and pulses for the FitzHugh–Nagumo PDE begins from the work of FitzHugh [22] (see also [34]) and includes the work on stability of Jones [25], Maginu [30], and Yanagida [43] (see also [29]), the work on existence of Deng [10] and existence and stability results of Evans [15, 16, 17, 18], Feroe [20], Wang [41, 42], Rinzel and Keller [35], and McKean [33] for the piecewise linear nonlinearity considered here.

This paper is organized as follows. In section 2 we present the model equations to be considered, including the nonlinearity, and derive traveling wave equations. In section 3, using transform techniques, we derive the general form for candidate front and pulse solutions. We consider one-front solutions in section 4 and show similarities with monotone one-front solutions of Nagumo type equations. In sections 5 and 6, using the form of the candidate solutions found in section 3, we derive conditions for the existence of one-pulse solutions. Two approaches are considered: one is perturbative in that it shows under certain conditions the existence of one-pulse solutions in a neighborhood of an existing one-pulse solution, while the other shows the existence of a one-pulse solution more directly, but with assumptions that are more difficult to verify. We present plots of the relationship between the driving force and the speed of wave propagation, and we present waveforms obtained numerically, in section 7.

2. Models. The continuous FitzHugh–Nagumo equations (the FH–N PDEs) can be derived as above by considering a smooth spatial domain (or a spatial scale where the local behavior appears homogenous) and thus allowing the spatial difference terms to go zero. This gives the model

$$(2.1) \quad \begin{cases} v_t = v_{xx} - f(v) - w, & x \in \mathbb{R}^N, t > 0, \\ w_t = b(v - rw), \end{cases}$$

where $b > 0$ relates the time scales of the pulse front and the recovery, the pulse's tail, and $r \geq 0$ indicates the strength of recovery.

In this paper we consider a differential-difference equation of FitzHugh–Nagumo type which contains both the diffusion term derived by considering periodically nodes, as in the introduction, and the diffusion term obtained by allowing the spatial domain to be uniform. While this may not be a valid first principle derivation, it does allow us to compare and contrast propagation of action potential in the two perspectives (allowing for different length scale assumptions). The equations of interest are

$$(2.2) \quad \begin{cases} \dot{v}(\eta, t) = \sum_{i=1}^N d_i L_i v(\eta, t) + \sum_{i=1}^N \gamma_i \frac{\partial^2 v}{\partial \eta_i^2}(\eta, t) - f(v(\eta, t)) - w(\eta, t), \\ \dot{w}(\eta, t) = b[v(\eta, t) - rw(\eta, t)], \end{cases}$$

for

- $\eta \in \mathbb{R}^N$, $t \in \mathbb{R}^+$, and η_i is the i th element of η ,
- “ \cdot ” denotes differentiation with respect to t ,
- $d_i \geq 0$, $\gamma_i \geq 0$, $i = 1, \dots, N$, $b > 0$, and $r \geq 0$ are parameters,
- $L_i v(\eta, t) = v(\eta + e_i, t) - 2v(\eta, t) + v(\eta - e_i, t)$, where e_i is the unit vector with 1 in the i th element, and
- in general, f is a function of “cubic” shape, but for our investigations, we employ the piecewise linear f (as was done in [33, 35, 20, 41, 42, 19, 7, 12, 13, 38, 39, 40]),

$$(2.3) \quad f(v) \equiv v - h(v - a), \quad \text{where} \quad h(v - a) \equiv \begin{cases} 0, & v < a, \\ [0, 1], & v = a, \\ 1, & v > a, \end{cases}$$

where $a \in (0, 1)$ is a “detuning” parameter allowing for tuning the behavior based on the behavior of the sodium channels.

While we have discussed only the derivation of the one-dimensional model of propagation along a single nerve axon, the equations presented in (2.2) are three-dimensional. This is simply a generalization we choose to explore and it may (or may not) be used to gain insight into three-dimensional biological domains such as cardiac tissue. We intend to study traveling waves (plane waves), and thus we now specify a direction of propagation with the direction normal $\sigma = \{\sigma_1, \dots, \sigma_N\}^T \in \mathbb{R}^N$, with $\sum_{i=1}^N \sigma_i^2 = 1$, and apply the classic traveling wave ansatz $\phi(\eta \cdot \sigma - ct) = v(\eta, t)$ and $\psi(\eta \cdot \sigma - ct) = w(\eta, t)$ to (2.2) to obtain the system of differential-difference equations:

$$(2.4) \quad \begin{cases} -c\phi'(\xi) = \sum_{i=1}^N d_i[\phi(\xi + \sigma_i) - 2\phi(\xi) + \phi(\xi - \sigma_i)] + \gamma\phi''(\xi) - f(\phi(\xi)) - \psi(\xi), \\ -c\psi'(\xi) = b[\phi(\xi) - r\psi(\xi)], \end{cases}$$

where $\gamma := \sum_{i=1}^N \gamma_i \sigma_i^2$ and c is the unknown wave speed.

3. Multiple pulse and front solutions. Although our interest in this paper is in one-pulse and one-front solutions, in this section we construct candidate solutions with any number of pulses or fronts, i.e., for $m \in \mathbb{Z}^+$ we construct

- m -pulse solutions where $\phi(-\infty) = \phi(+\infty) = 0$ and $\psi(-\infty) = \psi(+\infty) = 0$, homoclinic connections between constant stable equilibrium solution 0 of (2.4), and
- m -front solutions for $r > 0$ such that $\phi(-\infty) = 0$, $\phi(+\infty) = \frac{r}{1+r}$, and $\psi(-\infty) = 0$, $\psi(+\infty) = \frac{1}{1+r}$, heteroclinic connections between constant stable equilibrium solutions of (2.4) for $0 < a < \frac{r}{1+r}$.

Before we begin construction, using linear transforms, we now take a close look at the piecewise linear nonlinearity f and its effects and a close look at the characteristic equation of (2.4).

3.1. The nonlinearity. Because we intend to apply linear transforms to (2.4) we rewrite the piecewise linear nonlinearity as

$$(3.1) \quad f(\phi(\xi)) = \phi(\xi) - h(\phi(\xi) - a) = \phi(\xi) - \sum_{k=0}^n (-1)^k h(\xi - \xi_k),$$

where the ξ_k are the unknown values of ξ , where $\phi = a$, $\phi' \neq 0$, $n = 2m - 1$ for pulse solutions and $n = 2m - 2$ for front solutions. This implies that when finding a

m -pulse solution, one also needs to seek the values $\xi_0 < \xi_1 < \dots < \xi_{2m-1}$ such that $\phi(\xi_k) = a$ for $k = 0, 1, \dots, 2m - 1$ with

- $\phi(\xi) < a$ for $\xi < \xi_0$, for $\xi_k < \xi < \xi_{k+1}$ with k odd, and for $\xi > \xi_{2m-1}$; and
- $\phi(\xi) > a$ for $\xi_k < \xi < \xi_{k+1}$ with k even.

Similarly, for an m -front solution one also needs to seek $0 = \xi_0 < \xi_1 < \dots < \xi_{2m-2}$ where $\phi(\xi_k) = a$ for $k = 0, 1, \dots, 2m - 2$ with

- $\phi(\xi) < a$ for $\xi < \xi_0$ and for $\xi_k < \xi < \xi_{k+1}$ with k odd; and
- $\phi(\xi) > a$ for $\xi > \xi_{2m-2}$ and for $\xi_k < \xi < \xi_{k+1}$ with k even.

Because the solutions we seek are translationally invariant we pin down the solution by choosing $\xi_0 = 0$.

Remark 3.1. Due to the set-valued nature of the nonlinearity (2.3) and the corresponding Heaviside functions in (3.1) we have that from (2.4)

$$\lim_{\xi \rightarrow \xi_k^-} c\phi'(\xi) + \gamma\phi''(\xi) \neq \lim_{\xi \rightarrow \xi_k^+} c\phi'(\xi) + \gamma\phi''(\xi)$$

and

$$\begin{cases} -c\phi'(\xi_k) - \gamma\phi''(\xi_k) \in \sum_{i=1}^N d_i(\phi(\xi_k + \sigma_i) - 2\phi(\xi_k) + \phi(\xi_k - \sigma_i)) - f(\phi(\xi_k)) - \psi(\xi_k), \\ -c\psi'(\xi_k) = b(\phi(\xi_k) - r\psi(\xi_k)) \end{cases}$$

for $k = 0, 1, \dots, n$.

3.2. The characteristic equation. We consider connecting orbits, homoclinic and heteroclinic connections, between homogeneous equilibria. A central aspect is the eigenstructure of the linearization about these equilibrium solutions. In contrast with the case of continuous diffusion in which the characteristic equation is written in terms of a polynomial, in the case of discrete diffusion the characteristic equation is a transcendental equation with an infinite number of solutions. Three aspects are especially important:

- (i) that the equilibria are hyperbolic in the sense that there are not purely imaginary solutions to the characteristic equation;
- (ii) that the dominant eigenvalues, those with smallest real part among those with positive real part and those with largest real part among those with negative real part, possess a gap (up to complex conjugates in the case of dominant complex eigenvalue) in their real parts with respect to other eigenvalues; and
- (iii) whether the dominant eigenvalues are real or a complex conjugate pair.

To study the characteristic equation of (2.4) we begin by linearizing around a constant equilibrium solution such that $f(\phi) \neq a$ to obtain the following linear differential equation:

$$\begin{cases} -cx'(\xi) = \sum_{i=1}^N d_i(x(\xi + \sigma_i) - 2x(\xi) + x(\xi - \sigma_i)) + \gamma x''(\xi) - x(\xi) - y(\xi), \\ -cy'(\xi) = b(x(\xi) - ry(\xi)). \end{cases}$$

On substituting $x(\xi) = \kappa_1 \exp(\lambda\xi)$ and $y(\xi) = \kappa_2 \exp(\lambda\xi)$ we obtain

$$(3.2) \quad \begin{cases} -c\lambda x(\xi) = \sum_{i=1}^N d_i(\exp(\lambda\sigma_i) - 2 + \exp(-\lambda\sigma_i))x(\xi) + \gamma\lambda^2 x(\xi) - x(\xi) - y(\xi), \\ -c\lambda y(\xi) = b(x(\xi) - ry(\xi)). \end{cases}$$

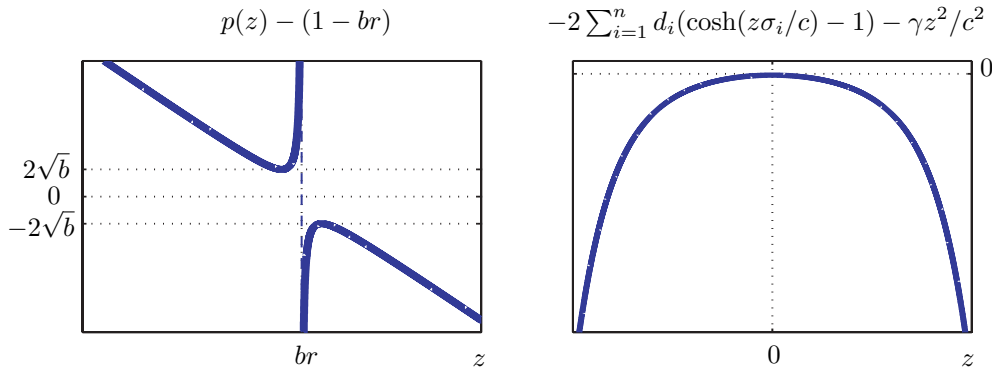


FIG. 3.1. On the left is a plot of the function $p(z) - (1 - br)$. To find the real roots of $p(z)$ one only needs to plot the constant valued function $br - 1$. On the right is a plot of $-2 \sum_{i=1}^n d_i (\cosh(z\sigma_i/c) - 1) - \gamma z^2/c^2$ when c is finite.

When $br \neq c\lambda$ the second equation of (3.2) is $y(\xi) = bx(\xi)/(br - c\lambda)$, which on substitution into the first equation of (3.2) yields the characteristic equation

$$(3.3) \quad \Delta(\lambda) := 1 - 2 \sum_{i=1}^n d_i (\cosh(\lambda\sigma_i) - 1) - \gamma\lambda^2 + \frac{b}{(br - c\lambda)} - c\lambda = 0.$$

Consider the change of variables $z = \lambda c$ and let $|c| \rightarrow \infty$. Then we have

$$p(z) = 0, \quad \text{where} \quad p(z) \equiv \lim_{|c| \rightarrow \infty} \Delta(z/c) = 1 + \frac{b}{(br - z)} - z.$$

For the following it may be illustrative to refer to Figure 3.1. Thus $p'(z) = b/(br - z)^2 - 1$, which equals zero when $z_{\pm} = br \pm \sqrt{b}$, one value on each side of the vertical asymptote $z = br$. The function p has a maximum of $p(z_+) = 1 - 2\sqrt{b} - br$ at $z_+ = br + \sqrt{b}$ and a minimum of $p(z_-) = 1 + 2\sqrt{b} - br$ at $z_- = br - \sqrt{b}$. Therefore, in the limit as $|c| \rightarrow \infty$, there are two positive real roots (greater than br) to the characteristic equation $\Delta(z/c)$ if $p(z_+) > 0$, i.e., if $r < (1 - 2\sqrt{b})/b$, and two positive real roots (less than br) in the limit if $p(z_-) < 0$, i.e., if $r > (1 + 2\sqrt{b})/b$. If $(1 - 2\sqrt{b})/b < r < (1 + 2\sqrt{b})/b$, then the roots in the limit are complex.

For c finite, the characteristic equation $\Delta(z/c) = p(z) - 2 \sum_{i=1}^n d_i (\cosh(z\sigma_i/c) - 1) - \gamma z^2/c^2$ always has one negative real root. If the roots in the limit are complex with positive real part, then for all finite c there will not be real positive roots to the characteristic equation. We are interested in cases where the characteristic equation does not admit purely imaginary or zero solutions. In this case the following lemma provides justification for our calculations.

LEMMA 3.1. *Let (ϕ, ψ) be a solution of (2.3), (2.4) for some $c \neq 0$. Then there exists $\delta_0 > 0$ such that for some $K > 0$,*

$$|\phi(\xi)| \leq Ke^{\delta_0 \xi}, \quad |\psi(\xi)| \leq Ke^{\delta_0 \xi}, \quad \text{for } \xi \leq 0.$$

Proof. The proof follows the proof of Lemma 4.1 of [7]; see also the proof of Lemma 3.1 of [13] and the proof of Lemma 2.1 of [12]. \square

3.3. Construction of candidate solutions. We are now ready to construct candidate solutions by employing the Fourier transform

$$\hat{\phi}_\delta(s) = \int_{-\infty}^{+\infty} e^{-is\xi} \phi_\delta(\xi) d\xi \quad \text{with} \quad \phi_\delta(\xi) = e^{-\delta\xi} \phi(\xi)$$

(and similarly for ψ) and $\delta > 0$ is sufficiently small. Convergence of the integral is guaranteed by Lemma 3.1, which implies that $\phi_\delta(\xi) \rightarrow 0$ and $\psi_\delta(\xi) \rightarrow 0$ exponentially fast, both as $\xi \rightarrow -\infty$ and $\xi \rightarrow +\infty$ for $0 < \delta < \delta_0$. Using (2.4) and (3.1) we have that $(\phi_\delta, \psi_\delta)$ satisfy

$$(3.4) \quad \left\{ \begin{aligned} (-c - 2\gamma\delta)\phi'_\delta(\xi) &= \sum_{i=1}^N d_i [e^{\delta\sigma_i} \phi_\delta(\xi + \sigma_i) - 2\phi_\delta(\xi) + e^{-\delta\sigma_i} \phi_\delta(\xi - \sigma_i)] + \gamma\ddot{\phi}_\delta(\xi) \\ &\quad - (1 - c\delta - \gamma\delta^2)\phi_\delta(\xi) + e^{-\delta\xi} \sum_{k=0}^n (-1)^k h(\xi - \xi_k) - \psi_\delta(\xi), \\ -c\psi'_\delta(\xi) &= b\phi_\delta(\xi) - [br - c\delta]\psi_\delta(\xi). \end{aligned} \right.$$

By applying the Fourier transform to (3.4) we obtain the following matrix equation:

$$M(s - i\delta) \begin{pmatrix} \hat{\phi}_\delta(\xi) \\ \hat{\psi}_\delta(\xi) \end{pmatrix} = \frac{1}{is + \delta} \begin{pmatrix} \sum_{k=0}^n (-1)^k e^{-is\xi_k} \\ 0 \end{pmatrix} \quad \text{with} \quad M(s) := \begin{pmatrix} R(s) & 1 \\ -b & B(s) \end{pmatrix},$$

where

$$(3.5) \quad R(s) = -cis + A(s), \quad A(s) = 1 + \gamma s^2 + 2 \sum_{i=1}^N d_i (1 - \cos(\sigma_i s)), \quad \text{and} \quad B(s) = -cis + br.$$

The matrix function $M(s)$ is invertible near the real axis. To see this note that we have $\det(M(s)) = R(s)B(s) + b$, and the imaginary part of the determinant is bounded away from zero for $s \neq 0$ near the real axis, while for $s = 0$ the real part of the determinant is bounded away from zero since $b > 0$ and $r \geq 0$.

Solving we obtain

$$\hat{\phi}_\delta(s) = \frac{B(s - i\delta)}{(is + \delta)[R(s - i\delta)B(s - i\delta) + b]} \sum_{k=0}^n (-1)^k e^{-is\xi_k}$$

and

$$\hat{\psi}_\delta(s) = \frac{b}{(is + \delta)[R(s - i\delta)B(s - i\delta) + b]} \sum_{k=0}^n (-1)^k e^{-is\xi_k},$$

and on applying the Fourier inversion theorem we obtain

$$(3.6) \quad \begin{aligned} \phi(\xi) &= e^{\delta\xi} \phi_\delta(\xi) = \frac{1}{2\pi} \int_{-\infty}^{+\infty} \hat{\phi}_\delta(s) e^{(is+\delta)\xi} ds \\ &= \frac{1}{2\pi i} \int_{-i\delta-\infty}^{-i\delta+\infty} \frac{B(s)}{s(R(s)B(s) + b)} \sum_{k=0}^n (-1)^k e^{is(\xi-\xi_k)} ds \\ &= \frac{1}{2\pi i} \left(\int_{C_\delta} + \int_{S_\delta} \right) \frac{B(s)}{s(R(s)B(s) + b)} \sum_{k=0}^n (-1)^k e^{is(\xi-\xi_k)} ds \end{aligned}$$

and

$$(3.7) \quad \psi(\xi) = e^{\delta\xi} \psi_\delta(\xi) = \frac{1}{2\pi i} \left(\int_{C_\delta} + \int_{S_\delta} \right) \frac{b}{s(R(s)B(s) + b)} \sum_{k=0}^n (-1)^k e^{is(\xi - \xi_k)} ds,$$

where C_δ denotes the two half-lines $(-\infty, -\delta]$ and $[\delta, \infty)$, and S_δ is the half-circle $t \rightarrow \delta e^{it}$ for $-\pi \leq t \leq 0$. Upon simplification, and taking $\delta \rightarrow 0$ we next obtain

$$(3.8) \quad \begin{aligned} \phi(\xi) &= \left(\frac{1 + (-1)^n}{4} \right) \left(\frac{r}{1+r} \right) + \int_0^\infty W(s) \sum_{k=0}^n (-1)^k \sin(s(\xi - \xi_k)) ds \\ &\quad + \int_0^\infty X(s) \sum_{k=0}^n (-1)^k \cos(s(\xi - \xi_k)) ds \quad \text{and} \\ \psi(\xi) &= \left(\frac{1 + (-1)^n}{4} \right) \left(\frac{1}{1+r} \right) + \int_0^\infty Y(s) \sum_{k=0}^n (-1)^k \sin(s(\xi - \xi_k)) ds \\ &\quad + \int_0^\infty Z(s) \sum_{k=0}^n (-1)^k \cos(s(\xi - \xi_k)) ds, \end{aligned}$$

where

$$(3.9) \quad W(s) = \frac{1}{\pi} \left[\frac{b^2 r + C(s)A(s)}{sD(s)} \right], \quad X(s) = \frac{c}{\pi} \left[\frac{-b + C(s)}{D(s)} \right],$$

$$(3.10) \quad Y(s) = \frac{b}{\pi} \left[\frac{brA(s) + b - c^2 s^2}{sD(s)} \right], \quad \text{and} \quad Z(s) = \frac{bc}{\pi} \left[\frac{A(s) + br}{D(s)} \right],$$

with $C(s) := b^2 r^2 + c^2 s^2$ and

$$D(s) := (R(s)B(s) + b)(R(-s)B(-s) + b) = c^2 s^2 (A(s) + br)^2 + (brA(s) - c^2 s^2 + b)^2.$$

Remark 3.2. The construction of candidate solutions is also applicable to more general diffusive operators. For example, consider for $N = 1$, the term (see also [3]) $\sum_{i=1}^N d_i(v(\eta + e_i, t) - 2v(\eta, t) + v(\eta - e_i, t)) + \sum_{i=1}^N \gamma_i \frac{\partial^2 v}{\partial \eta_i^2}(\eta, t)$ in (2.2) replaced by

$$d \left(-2v(\eta, t) + \sum_{j=1}^\infty \alpha_j \{v(\eta + j, t) + v(\eta - j, t)\} \right) + \gamma \frac{\partial^2 v}{\partial \eta_i^2}(\eta, t), \quad \sum_{j=1}^\infty \alpha_j = 1.$$

The main change to the derivation is that $A(s)$ in (3.5) becomes

$$A(s) = 1 + \gamma s^2 + 2d \sum_{j=1}^\infty \alpha_j (1 - \cos(js)).$$

4. Further discussion of one-front candidate solutions. The potential solutions derived in (3.8)–(3.10) are one-front solutions when $n = 0$. Notice that to satisfy the boundary conditions, the detuning parameter a must be restricted so that $a \in [0, r/(1+r)]$. From (3.8)–(3.10) we have the following symmetry property:

$$(4.1) \quad \phi(\xi, c) = \frac{r}{1+r} - \phi(-\xi, -c) \quad \text{and} \quad \psi(\xi, c) = \frac{1}{1+r} - \psi(-\xi, -c).$$

By (3.6) we have that $|\phi(\xi)| = O(e^{\delta\xi})$ as $\xi \rightarrow -\infty$, so the boundary condition $\phi(-\infty) = 0$ holds. By (4.1), $\phi(+\infty) = \frac{r}{1+r}$ and the boundary conditions for ψ are satisfied similarly using (3.7) and (4.1).

In certain limits the existence of one-front solutions is known. For instance, if we let $b = \epsilon$ in (2.4), then in the limit as $\epsilon \rightarrow 0$, $\psi(\xi) = \psi_0$, a constant, and we can then consider the Nagumo equation with nonlinearity $\tilde{f}(\phi) = f(\phi) - \psi_0$ provided $1 - a < \psi_0 < a$, in which case we seek a one-front solution such that $\phi(-\infty) = \psi_0$ and $\phi(+\infty) = 1 + \psi_0$. In this case previous results (see, e.g., [7]) concerning one-front solutions scaled so that $\tilde{\phi}(-\infty) = 0$ and $\tilde{\phi}(+\infty) = 1$ are applicable by considering a fixed ψ_0 and considering the correspondence $\phi(\xi) = \tilde{\phi}(\xi) + \psi_0$.

Similarly, if we let $r = 1/\epsilon$ and let $\epsilon \rightarrow 0$, then $\psi_0 = 0$ and results in [7] on propagation failure, monotonicity of one-front solutions, and monotonicity of the (a, c) relationship are directly applicable. Furthermore, we expect these behaviors to persist in a neighborhood of the limiting parameter value.

4.1. Verification of candidate one-front solution. First, we have assumed $\phi(0) = a$, so by (3.8),

$$(4.2) \quad a = \frac{1}{2} \left(\frac{r}{1+r} \right) + \int_0^\infty X(s) ds.$$

The candidate solution found in (3.8)–(3.10) is consistent with our ansatz of (3.1) with $n = 0$ provided $\phi(\xi) > a$ for $\xi > 0$ and $\phi(\xi) < a$ for $\xi < 0$, where ϕ is defined by (3.8) and a is defined in (4.2). Since the boundary conditions are satisfied, if the roots of the corresponding characteristic equation (3.3) do not lie on the imaginary axis, then for $|\xi|$ large enough the solution ϕ in (3.8) is bounded away from a . Thus it is enough to check $\phi(\xi) > a$ for $\xi > 0$ and $\phi(\xi) < a$ for $\xi < 0$ over a finite interval of values ξ . Clearly, we expect to have one-front solutions for $b \approx 0$ and for r large enough.

5. Further discussion of one-pulse candidate solutions. The derivation in section 3 relied on the assumption that there exists an m -pulse solution (or a front solution). This allowed us to write the nonlinear term as a linear term and a sum of Heaviside functions. In this section we give conditions under which these assumptions may be verified for one-pulse solutions.

Existence of ξ_1 . Our assumption for one-pulse solutions was that $\phi(0) = a$ and $\phi(\xi_1) = a$ for some $\xi_1 > 0$ and $\phi(\xi) < a$ for $\xi < 0$ and for $\xi > \xi_1$ with $\phi(\xi) > a$ for $0 < \xi < \xi_1$. Using the form of the candidate solutions (3.8), (3.9), and (3.10), to have $\phi(0) = \phi(\xi_1) = a$, there must be $\xi_1 > 0$ such that $g(\xi_1) = 0$, where

$$\int_0^\infty X(s)(2 - 2 \cos(s\xi)) ds = \frac{2c}{\pi} \int_0^\infty \frac{-b + C(s)}{D(s)} (1 - \cos(s\xi_1)) ds \equiv \frac{2c}{\pi} g(\xi).$$

The existence of such a $\xi_1 > 0$ that satisfies $g(\xi_1) = 0$ for $c \neq 0$ is a *necessary* condition for the existence a one-pulse solution to (2.3) and (2.4). Let

$$Q(s) = -b + C(s),$$

so we can write

$$(5.1) \quad g(\xi_1) = \int_0^\infty \frac{Q(s)}{D(s)} (1 - \cos(s\xi_1)) ds.$$

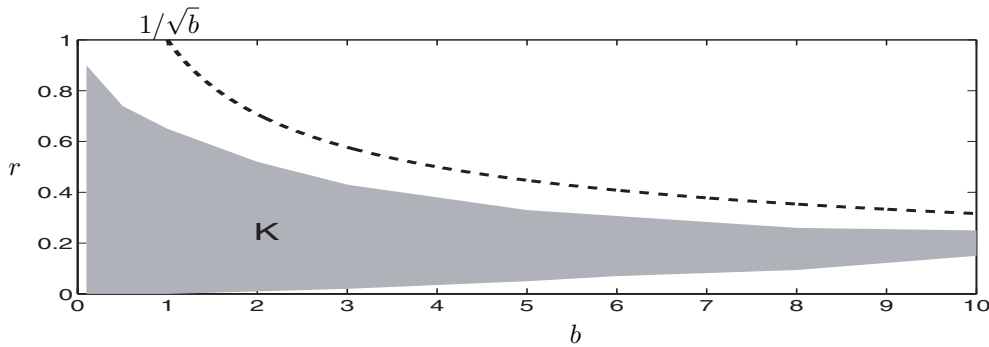


FIG. 5.1. In this example, the shaded area K indicates values of (b, r) which satisfy the conditions of Theorem 5.1. The dashed line is $br^2 = 1$. $N = \gamma = d_1 = c = 1$.

Remark 5.1. This same type of idea could be applied to verifying the existence of general m -pulse solutions. However, in that case, the existence of a zero for a system of $2m - 1$ equations in $2m - 1$ unknowns must be verified.

The idea behind the following theorem is to show that for $\xi_1 > 0$ g is positive for ξ_1 small and g is negative for ξ_1 large. It is motivated by the situation for the spatially continuous problem (2.1) with the piecewise linear nonlinearity (2.3). In the spatially continuous diffusion operator case, $D(s)$ is proportional to s^6 as $s \rightarrow \infty$ so that $g, g',$ and g'' are defined by absolutely convergent integrals.

THEOREM 5.1. *There exists a positive zero of g defined in (5.1) for wave speed $c \neq 0$ provided $br^2 < 1$,*

$$(5.2) \quad \int_0^\infty \frac{Q(s)}{D(s)} ds < 0,$$

and for all $\nu > 0$ sufficiently small

$$(5.3) \quad - \int_0^{s^*} s^2 \frac{Q(s)}{D(s)} ds < \int_{s^*}^\infty s^2 \frac{Q(s)}{D(s) + \nu s^6} ds,$$

where $s^* = \sqrt{\frac{b(1-br^2)}{c^2}}$.

The shaded region of Figure 5.1 illustrates values of (b, r) which satisfy the conditions of this theorem, for $N = \gamma = d_1 = c = 1$. They were verified by comparison, bounding $D(s)$ with functions of the form $c_1 s^6 + c_2 s^3 + c_3$.

Proof. We have $D(s) > 0$ for $s \geq 0$ and since $br^2 < 1$, $Q(s^*) = 0$, $Q(s) < 0$ for $s < s^*$, and $Q(s) > 0$ for $s > s^*$. We want to show that $g(\xi_1) > 0$ for $\xi_1 > 0$ sufficiently small and $g(\xi_1) < 0$ for $\xi_1 > 0$ sufficiently large.

To this end note that for any bounded continuous function κ defined for $s \geq 0$, for $x > 0$

$$\int_0^\infty \kappa(s) \cos(sx) ds = \int_0^\infty \frac{1}{x} \kappa(u/x) \cos(u) du \rightarrow 0 \quad \text{as } x \rightarrow \infty.$$

Thus, $g(\xi_1) < 0$ for $\xi_1 > 0$ sufficiently large follows from (5.2).

Next observe that $g(0) = 0$ and define

$$h(\xi_1) = \int_0^{s^*} \frac{Q(s)}{D(s)} (1 - \cos(s\xi_1)) ds + \int_{s^*}^\infty \frac{Q(s)}{D(s) + \nu s^6} (1 - \cos(s\xi_1)) ds.$$

Then

$$h'(\xi_1) = \int_0^{s^*} s \frac{Q(s)}{D(s)} \sin(s\xi_1) ds + \int_{s^*}^\infty s \frac{Q(s)}{D(s) + \nu s^6} \sin(s\xi_1) ds,$$

and so $h'(0) = 0$. Similarly,

$$h''(\xi_1) = \int_0^{s^*} s^2 \frac{Q(s)}{D(s)} \cos(s\xi_1) ds + \int_{s^*}^\infty s^2 \frac{Q(s)}{D(s) + \nu s^6} \cos(s\xi_1) ds,$$

and since for $s \geq s^*$, $Q(s) \geq 0$ and $(D(s) + \nu s^6)^{-1} < (D(s))^{-1}$, (5.3) implies that g is increasing for $\xi_1 = 0$, so that $g(\xi_1) > 0$ for $\xi_1 > 0$ sufficiently small. Thus, since g is continuous and changes sign at least once, there exists a $\xi_1 > 0$ such that $g(\xi_1) = 0$. \square

COROLLARY 5.1. *There exists a positive zero of g defined in (5.1) for wave speed $c \neq 0$ provided $br^2 < 1$ and either*

- (i) *for $d_1 = \dots = d_N = 0$ and $\gamma > 0$, (5.2) holds and (5.3) holds with $\nu = 0$, or*
- (ii) *for $d_j \geq 0$, with at least one $d_j > 0$, $j = 1, \dots, N$, and $\gamma = 0$, (5.2) holds.*

Proof. When $d_1 = \dots = d_N = 0$ and $\gamma > 0$, then the integral on the right-hand side of (5.3) is absolutely convergent with $\nu = 0$. However, for $d_j \geq 0$, with at least one $d_j > 0$, and $\gamma = 0$, the right-hand side of (5.3) approaches $+\infty$ as $\nu \rightarrow 0$, and so in this case (5.3) is always satisfied. \square

6. Existence of solutions. An important aspect of employing the McKean nonlinearity (2.3) is that (3.8)–(3.10) provide an explicit form (up to quadrature) for candidate solutions. This explicit form is useful in determining $\{\xi_k\}_k^n$ since for $\xi_0 = 0$ and $n \geq 1$, $\{\xi_k\}_k^n$ satisfies the system of nonlinear equations

$$(6.1) \quad \phi(0) - \phi(\xi_k) = 0, \quad k = 1, \dots, n,$$

and in subsequently verifying

$$(6.2) \quad (-1)^k (\phi(0) - \phi(\xi)) > 0, \quad \xi \in (\xi_{k-1}, \xi_k), \quad k = 0, \dots, n,$$

where we have set $\xi_{-1} = -\infty$ and $\xi_{n+1} = +\infty$. A necessary condition for (6.2) is that

$$(6.3) \quad (-1)^k \lim_{\xi \rightarrow \xi_k \pm} \phi'(\xi) > 0,$$

which for $c > 0$ involves only a one-sided limit since

$$(6.4) \quad (-1)^k \lim_{\xi \rightarrow \xi_k^-} \phi'(\xi) > (-1)^k \lim_{\xi \rightarrow \xi_k^+} \phi'(\xi).$$

One needs only to determine if the inequalities (6.2) are satisfied outside a neighborhood of $\{\xi_k\}_{k=1}^n$ if (6.3) holds.

The existence of $\{\xi_k\}_{k=0}^n$ is trivial for one-front solutions, $n = 0$, since we may choose $\xi_0 = 0$ by translation invariance, while for one-pulse solutions, $n = 1$, Theorem 5.1 and Corollary 5.1 provide criteria for the existence of $\xi_1 > 0$. In general for $n \geq 2$ establishing the existence of $\{\xi_k\}_k^n$ such that (6.1) holds is more difficult since this results in a nonlinear system of $n \geq 2$ equations in n unknowns. In the case of $n \geq 2$ perturbation/continuation techniques are more promising. One-front ($n = 0$) and one-pulse ($n = 1$) solutions provide building blocks for more general $n \geq 2$ solutions.

We are interested in connecting orbits between hyperbolic equilibria in which there is gap between

- (1) the dominant solution(s) to the characteristic equation
- (2) and the rest of the solutions to the characteristic equation.

The following lemmas show that for the characteristic equation (3.3) of (2.4) with (2.3) with $N = 1$, $d_1 = d > 0$, and $\gamma = 0$

- there are no purely imaginary solutions
- and if $\sinh((1 + 2d - \sqrt{4d^2 + c^2})/c) \neq -c/(2d)$, then all the solutions are simple.

LEMMA 6.1. *Let λ_1, λ_2 denote two solutions to the characteristic equation (3.3). Write $\lambda_j = a_j + ib_j$ for $j = 1, 2$ and let $c > 0$ be given. If $(br - ca_1)^2 + (cb_j)^2 > 0$ for $j = 1, 2$, then $a_1 = a_2$ implies $b_1 = \pm b_2$.*

Proof. We have that λ_j is a solution of the characteristic equation provided

$$\begin{aligned} (br - ca_j)R_j + cb_jI_j &= 0, & R_j &= 1 - 2d(\operatorname{Re}(\cosh(\lambda_j)) - 1) - ca_j, \\ \text{where} & & & \\ -cb_jR_j + (br - ca_j)I_j &= 0, & I_j &= -2d(\operatorname{Im}(\cosh(\lambda_j))) - cb_j, \end{aligned}$$

for $j = 1, 2$. Thus, if $a_1 = a_2$ and $(br - ca_1)^2 + (cb_j)^2 > 0$, then $R_j = 0$ and $I_j = 0$ for $j = 1, 2$, and so

$$(6.5) \quad 1 - 2d(\cos(b_j) \cosh(a_j) - 1) - ca_j = 0, \quad -2d \sin(b_j) \sinh(a_j) - cb_j = 0$$

for $j = 1, 2$. Using the first equation in (6.5), if $a_1 = a_2$, then $\cos(b_1) = \cos(b_2)$, and so $\sin(b_1) = \pm \sin(b_2)$. If $\sin(b_1) = \sin(b_2)$, then the second equation in (6.5) implies that $c(b_1 - b_2) = 0$, and if $\sin(b_1) = -\sin(b_2)$, then the second equation in (6.5) gives $c(b_1 + b_2) = 0$. \square

LEMMA 6.2. *If $c > 0$, $b > 0$, $r \geq 0$, and $d > 0$, then any root $\lambda = x + iy$ of (3.3) has $x \neq 0$.*

Proof. If we write $\Delta(\lambda) = 0$ as $N(\lambda) + b/(br - c\lambda) = 0$, then $r = 0$ implies $\lambda \neq 0$. If $r > 0$ and $\lambda = 0$ is a solution, then $N(0) + 1/r = 0$, so $1 - 2d(\cos(0) - 1) + 1/r = 0$, which cannot occur for $r > 0$. If $x = 0$, but $y \neq 0$, then by the argument in the proof of Lemma 6.1, $\operatorname{Re}(N(\lambda)) = 0$ and $\operatorname{Im}(N(\lambda)) = 0$, so we have $1 + 2d - \cos(y) = 0$ and $-cy = 0$, which cannot both be simultaneously satisfied. \square

LEMMA 6.3. *If for $c > 0$ and $d > 0$ one has $\sinh((1 + 2d - \sqrt{4d^2 + c^2})/c) \neq -c/(2d)$, then there does not exist a double root to (3.3) for λ not purely imaginary.*

Proof. If there is a double root, λ , then $\Delta(\lambda) = 0$ and $\Delta'(\lambda) = 0$. Write $\Delta(\lambda)$ as $N(\lambda) + b/(br - c\lambda)$, so $\Delta'(\lambda) = N'(\lambda) + cb/(br - c\lambda)^2$. Thus, $\Delta'(\lambda) = N'(\lambda) + \frac{c}{b}N^2(\lambda)$, so by the argument in the proof of Lemma 6.1, $\operatorname{Re}(N(\lambda)) = 0$ and $\operatorname{Im}(N(\lambda)) = 0$, and if there is a double root, then $\Delta'(\lambda) = N'(\lambda) = 0$. Then for $\lambda = x + iy$, $-2d \cos(y) \sinh(x) - c = 0$ and $-2d \sin(y) \cosh(x) = 0$, we have $\sin(y) = 0$, and since $\operatorname{Im}(N(\lambda)) = 0$, we have $-2d \sin(y) \sinh(x) - cy = 0$, so $y = 0$. Thus, $-2d \sinh(x) - c = 0$, which implies $\sinh(x) = -c/(2d)$ and $\cosh(x) = \sqrt{4d^2 + c^2}/(2d)$. Hence, the only way for $\operatorname{Re}(N(\lambda)) = 0$ is if $x = (1 + 2d - \sqrt{4d^2 + c^2})/c$. \square

6.1. Existence of one-pulse solutions. Given existence of $\xi_1 > 0$ such that $g(\xi_1) = 0$ for g in (5.1), we now turn our attention to showing existence of one-pulse solutions. We proceed in two ways: in the first we assume the existence at a particular value of the wave speed c and then show existence (under certain conditions) in a neighborhood (Theorem 6.4); in the second we verify that $\phi(\xi) < a$ only when $\xi < 0$ and $\xi > \xi_1$ ($\phi(\xi) > a$ for $\xi \in (0, \xi_1)$) and then show that this condition can in certain cases be reduced to checking on finite intervals (Theorems 6.5 and 6.6).

THEOREM 6.4. *Suppose for fixed values of the parameters and $(a, c) = (a^*, c^*)$ with $c^* > 0$ we have a one-pulse solution defined for $\xi_1 > 0$ such that*

$$(6.6) \quad \text{for } \xi \in (0, \xi_1), \phi(\xi) - \phi(0) > 0, \quad \text{for } \xi < 0 \text{ and } \xi > \xi_1, \phi(\xi) - \phi(0) < 0,$$

$$(6.7) \quad \lim_{\xi \rightarrow 0^\pm} \phi'(\xi) > 0 \text{ and } \lim_{\xi \rightarrow \xi_1^\pm} \phi'(\xi) < 0,$$

and

$$(6.8) \quad 0 < \left| \int_0^\infty \frac{sQ(s)}{D(s)} \sin(s\xi_1) ds \right| < \infty.$$

Then for all c in a neighborhood of c^* there exist one-pulse solutions to (2.3), (2.4).

Proof. We argue by the implicit function theorem. We need to show that ξ_1 depends smoothly on c . This follows from (6.8) since by direct calculation

$$(6.9) \quad \xi_1'(c) = - \frac{\int_0^\infty \frac{Q_1(s)}{D^2(s)} (1 - \cos(s\xi_1)) ds}{\int_0^\infty \frac{sQ(s)}{D(s)} \sin(s\xi_1) ds},$$

where $Q_1(s) = Q_c(s)D(s) - Q(s)D_c(s)$ and Q_c and D_c are the derivatives of Q and D with respect to c , respectively. Now by the implicit function theorem, (6.6) and (6.7) hold in a neighborhood of c^* since the derived solution (3.8)–(3.10) and the one-sided derivatives at $\xi = 0$ and $\xi = \xi_1$ depend smoothly on ξ_1 and c . \square

Inequalities (6.2), when satisfied over the entire real line, imply existence; see Theorem 6.5. Lemmas 6.1–6.3 that show the hyperbolicity of the equilibria and the gap condition are used to show that is sufficient to check these inequalities over a certain finite interval; see Theorem 6.6.

THEOREM 6.5. *If $g(\xi_1) = 0$ for $\xi_1 > 0$ and*

$$(6.10) \quad \int_0^\infty W(s)[\sin(s(\xi_1 + \delta)) - \sin(s\delta) - \sin(s\xi_1)] ds < \left| \int_0^\infty X(s)[\cos(s(\xi_1 + \delta)) - \cos(s\delta)] ds \right|,$$

if $\delta > 0$,

$$(6.11) \quad - \int_0^\infty W(s)[\sin(s(\xi_1 + \delta)) - \sin(s\delta) - \sin(s\xi_1)] ds < \int_0^\infty X(s)[\cos(s(\xi_1 + \delta)) - \cos(s\delta)] ds,$$

if $-\xi_1 < \delta < 0$, then there exists a one-pulse solution to (2.3), (2.4).

Proof. We assume there exists a positive zero, ξ_1 , of g . Then for this $\xi_1 > 0$ we have $\phi(0) = a$ and $\phi(\xi_1) = a$. We show that (6.10) implies that $\phi(\xi) < a$ for $\xi < 0$ and $\xi > \xi_1$ and (6.11) implies $\phi(\xi) > a$ for $0 < \xi < \xi_1$. Recalling that $g(\xi_1) = 0$ implies $\int_0^\infty X(s)(1 - \cos(s\xi_1)) ds = 0$ along with the solution equalities (3.8)–(3.10), (6.10) can be rewritten as

$$-\phi(0) < -\phi(-\delta) \quad \text{and} \quad -\phi(0) < -\phi(\delta + \xi_1), \quad \delta > 0,$$

which implies $\phi(\xi) < a \equiv \phi(0)$ for $\xi < 0$ and for $\xi > \xi_1$. Similarly (6.11) can be rewritten as

$$\phi(0) < \phi(\delta + \xi_1), \quad -\xi_1 < \delta < 0,$$

which implies $\phi(\xi) > a \equiv \phi(0)$ for $0 < \xi < \xi_1$. \square

THEOREM 6.6. *Suppose for some value $c > 0$ and all other parameter values fixed there exists $\xi_1 > 0$ such that $g(\xi_1) = 0$. Suppose that the characteristic equation (3.3) has no solutions on the imaginary axis and order the solutions with positive real parts by the real parts: $\text{Re}(\lambda_1^+) \leq \text{Re}(\lambda_2^+) \leq \text{Re}(\lambda_3^+) \leq \dots$ and similarly for the solutions with negative real parts as: $\text{Re}(\lambda_1^-) \geq \text{Re}(\lambda_2^-) \geq \text{Re}(\lambda_3^-) \geq \dots$. If $\lambda_1^+ = \bar{\lambda}_2^+$ assume $\epsilon_0^+ := \text{Re}(\lambda_3^+) - \text{Re}(\lambda_2^+) > 0$. If $\lambda_1^+ \neq \bar{\lambda}_2^+$ assume $\epsilon_0^+ := \text{Re}(\lambda_2^+) - \text{Re}(\lambda_1^+) > 0$. Similarly, assume $\epsilon_0^- > 0$ for the solutions with negative real parts. Then there exist $T^+ > 0$ and $T^- < 0$ such that (6.10) and (6.11) need only be checked on $(0, T^+)$ and $(0, -T^-)$, respectively.*

Proof. Consider (3.6) and observe that if $\lambda \in \mathbb{C}$ is a solution of the characteristic equation (3.3), then $-i\lambda$ is a zero of $R(s) + b/B(s)$ in (3.6). First assume that $0 < \epsilon^+ < \epsilon_0^+$ and shift the contour in (3.6) from $\text{Im } s = -\delta$ to $\text{Im } s = -(\text{Re}(\lambda_1^+) + \epsilon^+)$. Then there are two cases: $\lambda_1^+ = \bar{\lambda}_2^+$ and $\lambda_1^+ \neq \bar{\lambda}_2^+$. If $\lambda_1^+ = \bar{\lambda}_2^+$, then we obtain

$$\begin{aligned} \phi(\xi) &= -\frac{B(s)\{e^{is\xi} - e^{is(\xi-\xi_1)}\}}{s(R'(s)B(s) + R(s)B'(s))}\Big|_{s=-i\lambda_1^+} - \frac{B(s)\{e^{is\xi} - e^{is(\xi-\xi_1)}\}}{s(R'(s)B(s) + R(s)B'(s))}\Big|_{s=-i\lambda_2^+} \\ &\quad + \frac{1}{2\pi i} \int_{-i(\text{Re}(\lambda_1^+) + \epsilon^+) - \infty}^{-i(\text{Re}(\lambda_1^+) + \epsilon^+) + \infty} \frac{B(s)\{e^{is\xi} - e^{is(\xi-\xi_1)}\}}{s(R(s)B(s) + b)} ds \\ &= C^+ \{e^{\lambda_1^+ \xi} - e^{\lambda_1^+ (\xi-\xi_1)}\} + O(e^{(\lambda_1^+ + \epsilon^+) \xi}) \end{aligned}$$

as $\xi \rightarrow -\infty$. Observe that

$$C^+ = -\frac{B(s)}{s(R'(s)B(s) + R(s)B'(s))}\Big|_{s=-i\lambda_1^+} - \frac{B(s)}{s(R'(s)B(s) + R(s)B'(s))}\Big|_{s=-i\lambda_2^+}.$$

If $\lambda_1^+ \neq \bar{\lambda}_2^+$ (and λ_1^+, λ_2^+ real), then we obtain

$$\begin{aligned} \phi(\xi) &= -\frac{B(s)\{e^{is\xi} - e^{is(\xi-\xi_1)}\}}{s(R'(s)B(s) + R(s)B'(s))}\Big|_{s=-i\lambda_1^+} \\ &\quad + \frac{1}{2\pi i} \int_{-i(\lambda_1^+ + \epsilon^+) - \infty}^{-i(\lambda_1^+ + \epsilon^+) + \infty} \frac{B(s)\{e^{is\xi} - e^{is(\xi-\xi_1)}\}}{s(R(s)B(s) + b)} ds \\ &= C^+ \{e^{\lambda_1^+ \xi} - e^{\lambda_1^+ (\xi-\xi_1)}\} + O(e^{(\lambda_1^+ + \epsilon^+) \xi}) \end{aligned}$$

as $\xi \rightarrow -\infty$, where $C^+ = -\frac{B(s)}{s(R'(s)B(s) + R(s)B'(s))}\Big|_{s=-i\lambda_1^+}$. Thus, there exists $T^- < 0$ such that $\phi(\xi) < \phi(0) =: a$ for $\xi \leq T^-$.

The argument for solutions to the characteristic equation (3.3) with negative real parts is treated similarly by moving the contour up. \square

7. Numerical results. In this section we present numerical results obtained by numerical integration of (3.8)–(3.10) and for one-pulse solutions by determining the positive zeros of (5.1). We approximate the integrals using the adaptive Gaussian quadrature code `adapt` of [37] after truncation to the interval $[0, 10^6]$. To find zeros of g we use the combined secant/bisection code `zero` of [37]. We focus on one-front, one-pulse, and two-pulse solutions, exhibit (a, c) curves, and waveforms of (3.8)–(3.10) with both continuous and discrete diffusion.

7.1. (a, c) curves. In Figure 7.1 we plot (a, c) curves for one-front solutions by approximating (4.2). We set $N = d_1 = d = 1$ and $\gamma = 0$ and vary b and r .

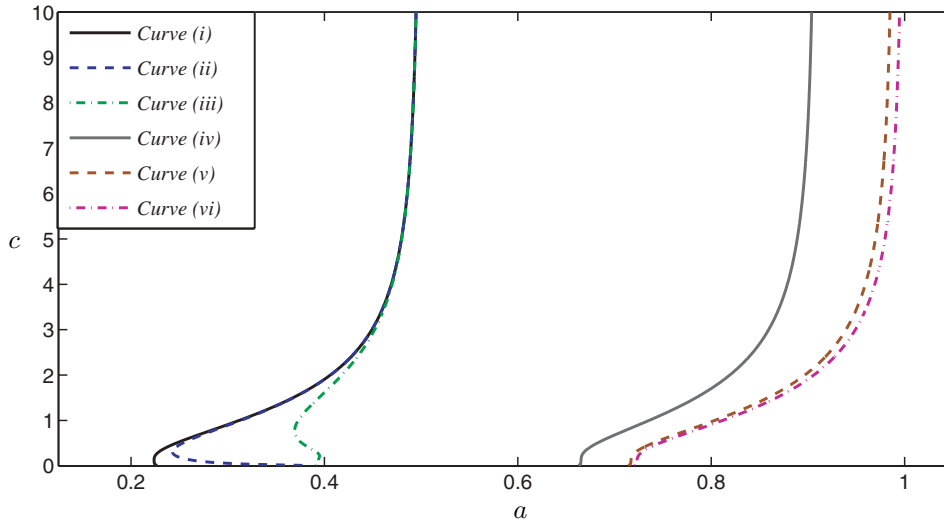


FIG. 7.1. Plot of (a, c) curves (moving from left to right) for (i) $(d, \gamma, b, r) = (1, 0, 10^{-4}, 1)$, (ii) $(d, \gamma, b, r) = (1, 0, 10^{-2}, 1)$, (iii) $(d, \gamma, b, r) = (1, 0, 1, 1)$, (iv) $(d, \gamma, b, r) = (1, 0, 1, 10^1)$, (v) $(d, \gamma, b, r) = (1, 0, 1, 10^2)$, and (vi) $(d, \gamma, b, r) = (1, 0, 0, 0)$, the discrete Nagumo equation.

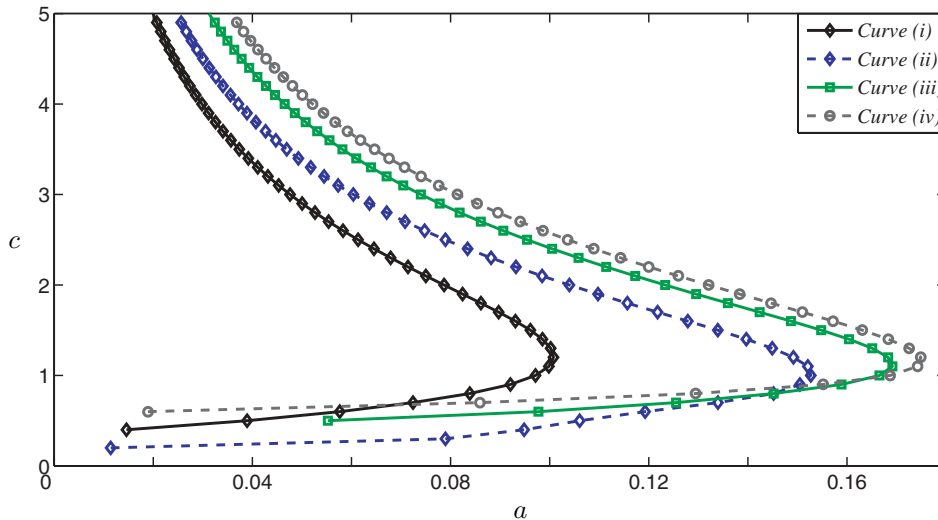


FIG. 7.2. Plot of (a, c) curves (moving from left to right) for (i) $(d, \gamma, b, r) = (1, 0, 1, 0)$, (ii) $(d, \gamma, b, r) = (0.8, 0.2, 1, 0)$, (iii) $(d, \gamma, b, r) = (0.4, 0.6, 1, 0)$, and (iv) $(d, \gamma, b, r) = (0, 1, 1, 0)$.

Notice the nonuniqueness suggested for $(b, r) = (10^{-2}, 1)$ and $(b, r) = (1, 1)$. The curves limit to $r/(r + 1)$ as $c \rightarrow \infty$. In Figure 7.2 we plot (a, c) curves for one-pulse solutions (these are actually (a, c) curves obtained when there exists $\xi_1 > 0$ such that $g(\xi_1) = 0$) for various values of the parameters d, γ, b, r . The plot illustrates the difference between the behavior with continuous and discrete diffusion. In the case of continuous diffusion it is known that the fast waves, i.e., those above the tip on the (a, c) curve, are stable (see [43, 30, 25, 29]), while the slow waves (those below the tip)

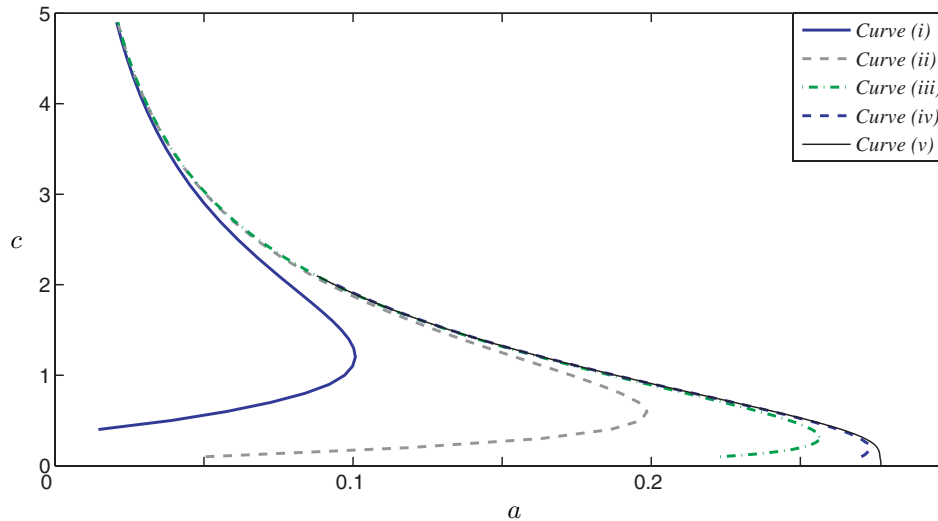


FIG. 7.3. Plot of (a, c) curves (moving from left to right) for (i) $(d, \gamma, b, r) = (1, 0, 1, 0)$, (ii) $(d, \gamma, b, r) = (1, 0, 10^{-1}, 0)$, (iii) $(d, \gamma, b, r) = (1, 0, 10^{-2}, 0)$, (iv) $(d, \gamma, b, r) = (1, 0, 10^{-3}, 0)$, and the limiting (a, c) curve obtained from the discrete Nagumo equation.

are unstable. In Figure 7.3 we highlight the dependence of the (a, c) relationship on the parameter $b > 0$ and compare it with the limiting (a, c) curve obtained from the discrete Nagumo equation, i.e., $b = 0$. Notice how the range of propagation failure in the discrete Nagumo equation limits tip of the (a, c) curve. The range of propagation failure limits the size of a for which there are one pulse solutions. Observe the larger values of a that are possible when b is small and the larger values of a obtained for the plot of the continuous (a, c) curve with $\gamma = 1$ as compared to the discrete for $d = 1$. In Figure 7.4 we vary the parameter $r > 0$. We set $b = 1$ and then have the requirement from Theorem 5.1 that $r^2 < 1$. In the plot for $r > 0$ there is an upper bound in c as well as a lower bound in c on the (a, c) curve.

7.2. Waveforms. In Figure 7.5 we plot one-front waveforms $\phi(\xi)$ and $\psi(\xi)$ fixing $(d, c, \gamma) = (1, 1, 0)$ and varying (b, r) . In Figure 7.6 we plot one-pulse waveforms $\phi(\xi)$ and $\psi(\xi)$ fixing $(b, r) = (1, 0)$, setting $(d, \gamma) = (1, 0)$, and varying the wavespeed c . Refer to Figure 7.2 for the parameter values in the (a, c) curve. The plot for $c = 0.6$ does not satisfy our assumption of a one-pulse solution since it violates $\phi(\xi) < a$ for $\xi > \xi_1$. Note, however, that $c = 0.6$ is one of the smaller values of c obtained in the (a, c) curve in Figure 7.2. In Figure 7.7 we plot waveforms $\phi(\xi)$ and $\psi(\xi)$ fixing $(b, r) = (1, 0)$, setting $(d, \gamma) = (0, 1)$, and varying the wavespeed c . The waveforms for the continuous operator are smooth compared to the waveforms for the discrete operator especially for small wavespeeds. The two-pulse solution in Figure 7.8 is obtained by superimposing two identical one-pulse solutions, using the superimposed one-pulse solutions as an initial guess and then applying Newton's method. The one-pulse solution is obtained from $(d, \gamma, c, b, r) = (1, 0, 1, 1, 0)$ and the pulses are put at a distance (in ξ) of 40 units apart. The value of a is slightly perturbed from the value of a for the one-pulse as one might expect (see [41]). In Figure 7.9 we plot the dependence of the parameter a on the distance between the pulses, $\xi_2 - \xi_1$, and compare with the value of a obtained for the one-pulse solution.

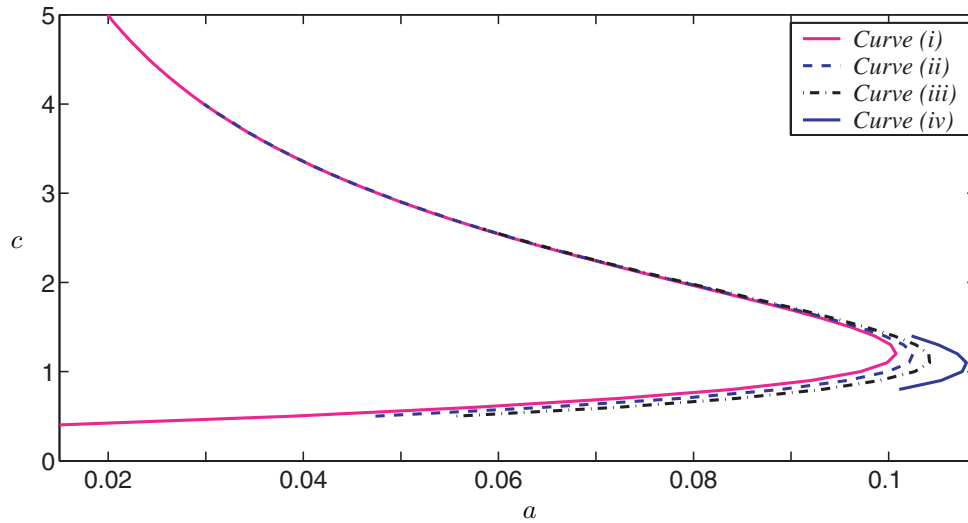


FIG. 7.4. Plot of (a, c) curves (moving from left to right) for (i) $(d, \gamma, b, r) = (1, 0, 1, 0)$, (ii) $(d, \gamma, b, r) = (1, 0, 1, 1/16)$, (iii) $(d, \gamma, b, r) = (1, 0, 1, 1/8)$, and (iv) $(d, \gamma, b, r) = (1, 0, 1, 1/4)$.

Front Solutions

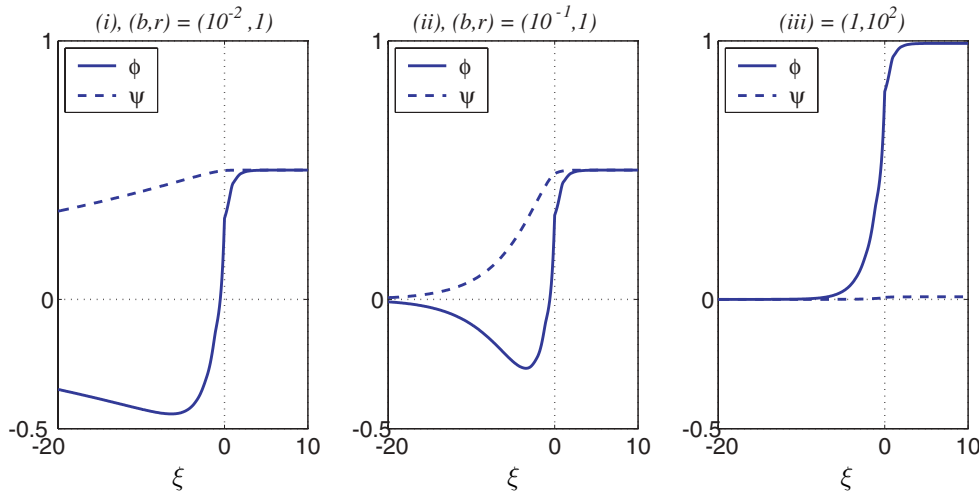


FIG. 7.5. Plot of one-front waveforms $\phi(\xi)$ and $\psi(\xi)$ for fixed $(d, c, \gamma) = (1, 1, 0)$, and (i) $(b, r) = (10^{-2}, 1)$, (ii) $(b, r) = (10^{-1}, 1)$, and (iii) $(b, r) = (1, 10^2)$.

7.3. Mixed continuous/discrete model. As an example of a model with continuous diffusion in one direction and discrete diffusion in the other coordinate direction we consider (2.2) with $N = 2$, $d_1 = d$, $d_2 = 0$, and $\gamma_1 = 0$, $\gamma_2 = \gamma$. Consider the direction of propagation $\sigma \in \mathbb{R}^2$ such that $\|\sigma\|_2 = 1$, and apply the traveling wave ansatz $u(\eta, t) = \phi(\eta \cdot \sigma - ct)$ and $w(\eta, t) = \psi(\eta \cdot \sigma - ct)$ to obtain (see (2.4))

$$(7.1) \quad \begin{cases} -c\phi'(\xi) = d(\phi(\xi + \sigma_1) - 2\phi(\xi) + \phi(\xi - \sigma_1)) + \gamma\sigma_2^2\phi''(\xi) - f(\phi(\xi)) - \psi(\xi), \\ -c\psi'(\xi) = b(\phi(\xi) - r\psi(\xi)). \end{cases}$$

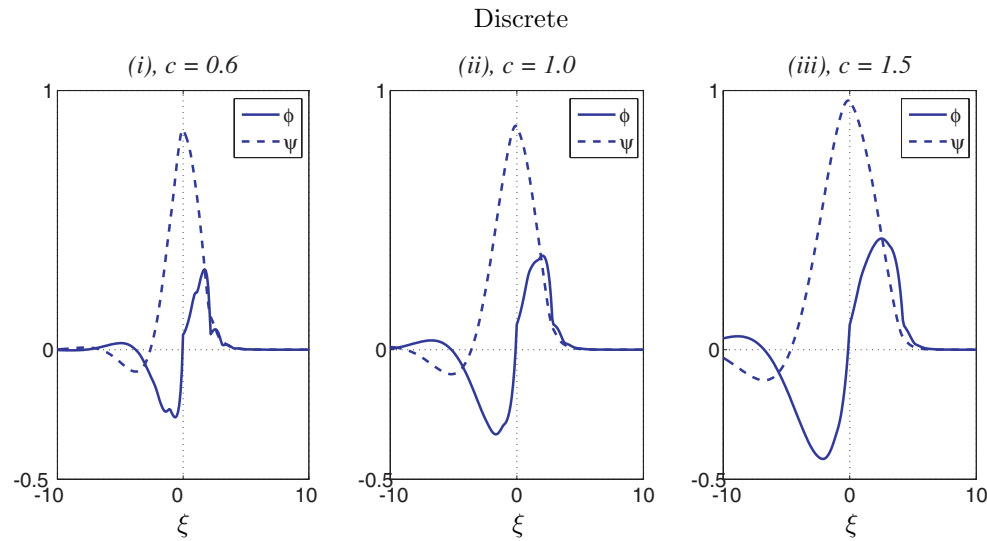


FIG. 7.6. *Discrete.* Plot of waveforms for fixed $(b, r) = (1, 0)$, and (i) $(d, \gamma, c) = (1, 0, 0.6)$, (ii) $(d, \gamma, c) = (1, 0, 1)$, (iii) $(d, \gamma, c) = (1, 0, 1.5)$.

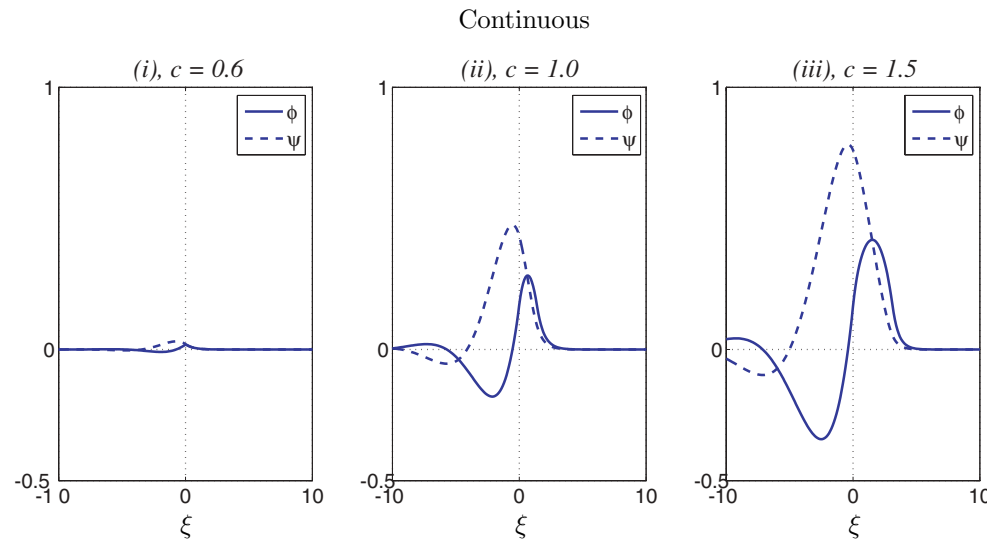


FIG. 7.7. *Continuous.* Plot of waveforms for fixed $(b, r) = (1, 0)$, and (i) $(d, \gamma, c) = (0, 1, 0.6)$, (ii) $(d, \gamma, c) = (0, 1, 1)$, (iii) $(d, \gamma, c) = (0, 1, 1.5)$.

If we rescale variables $x = \xi/\sigma_1$ and $\tilde{c} = c/\sigma_1$, then (7.1) becomes

$$(7.2) \quad \begin{cases} -\tilde{c}\phi'(x) = d(L\phi)(x) + g\phi''(x) - f(\phi(x)) - \psi(x), \\ -\tilde{c}\psi'(x) = b(\phi(x) - r\psi(x)), \end{cases}$$

where $g = \gamma \frac{\sigma_2^2}{\sigma_1^2}$ for $\sigma_1 \neq 0$ and $(L\phi)(x) = \phi(x + 1) - 2\phi(x) + \phi(x - 1)$.

In Figure 7.10 we set $(d, \gamma, b, r) = (1, 1, 1, 0)$ and $(d, \gamma, b, r) = (1, 0, 1, 0)$, set $c = 1$ and $c = 2$, let $\sigma_1 = \cos(\theta)$ and $\sigma_2 = \sin(\theta)$ for $0 \leq \theta \leq 2\pi$. The plot in Figure 7.10(i)

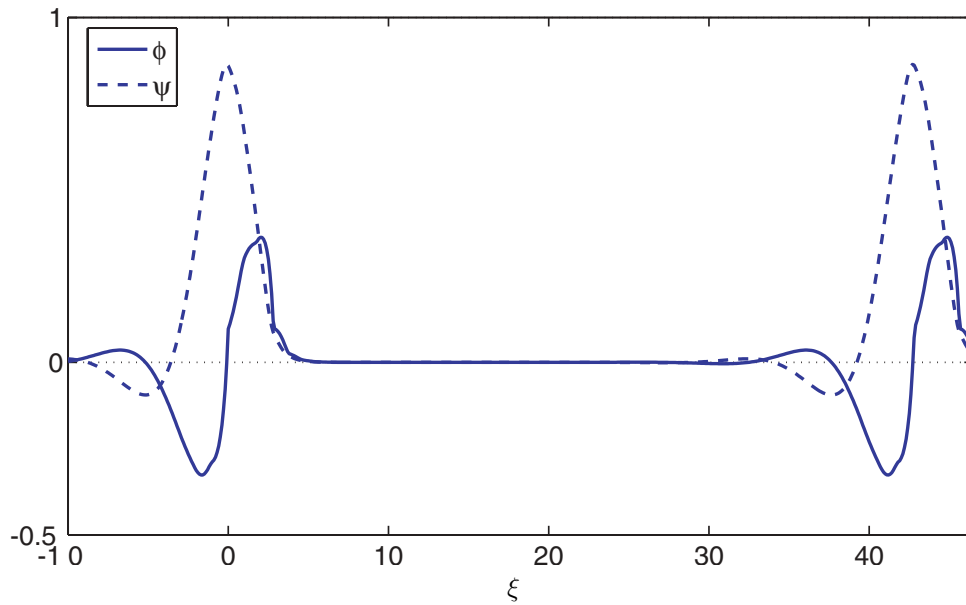


FIG. 7.8. Plot of two-pulse waveforms for $(d, c, \gamma, b, \tau) = (1, 1, 0, 1, 0)$ obtained as a perturbation of a superposition of two identical one-pulse solutions.

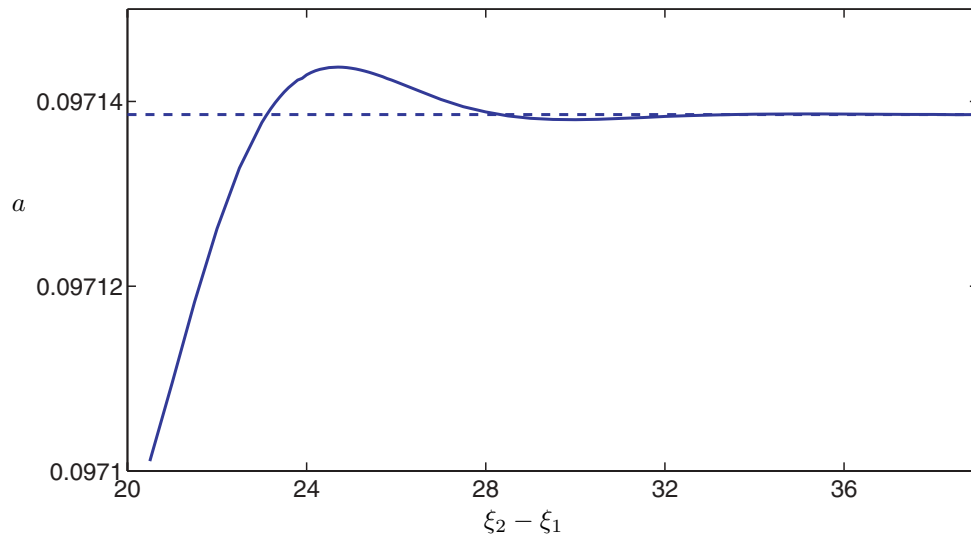


FIG. 7.9. Plot of computed a obtained for $(d, c, \gamma, b, \tau) = (1, 1, 0, 1, 0)$ as a function the distance between the two pulses, $\xi_2 - \xi_1$, and compared with the horizontal line, the computed a value for the one-pulse solution.

is a polar plot of a versus θ for the mixed continuous/discrete model and what we observed is that smaller values of a are obtained for $\sigma_1 \approx 1$ and compared with $\sigma_1 \approx 0$. This may be compared with the lack of anisotropy for the continuous model in Figure 7.10(ii) and the four-fold symmetry for the discrete model in Figure 7.10(iii).

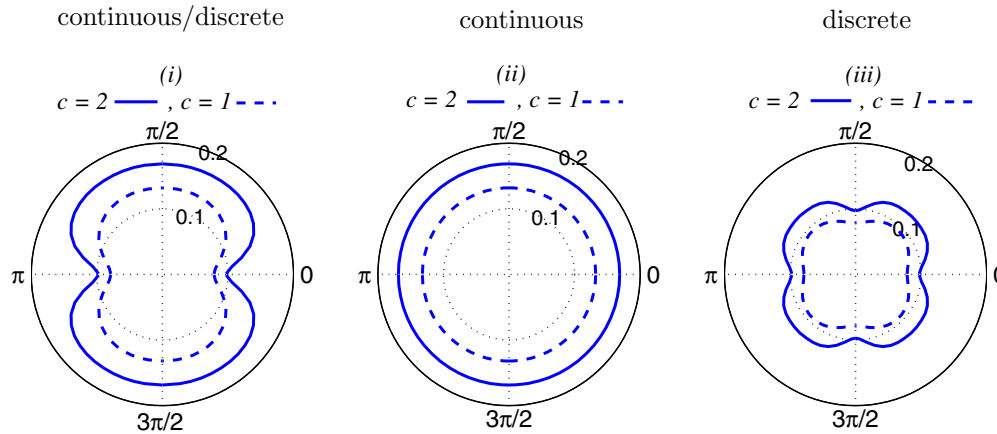


FIG. 7.10. Polar plot of $(\theta, a(\theta))$ for $(b, r) = (1, 0)$; see (7.2). In plot (i) $(d, g) = (1, 1)$ with $c = 2$ and $c = 1$ for the mixed continuous/discrete version of the equation, in plot (ii) $(d, g) = (0, 1)$ with $c = 2$ and $c = 1$ for the continuous version of the equation, and in plot (iii) $(d, g) = (1, 0)$ with $c = 2$ and $c = 1$ for the discrete version of the equation.

8. Conclusion. For a particular version of the FitzHugh–Nagumo equation (one which includes both spatially discrete and spatially continuous diffusive operators) with the McKean nonlinearity describing excitability, we have demonstrated how to construct candidate traveling wave solutions and have given tools for verifying if they are indeed solutions. This equation is meant to include models of action potential propagation on several length scales, from the internodal scale to the scale where a pulse becomes a spike. We begin by discussing the infinite number of eigenvalues obtained from linearizing. Leading edge behavior is governed by real eigenvalues, pulse trailing tails by complex ones (with nonzero real parts). Since solutions approach fixed points exponentially as we approach either plus or minus infinity, we can and do use the Fourier transform to derive candidate solutions. The one-front solutions (no recovery) we find have appeared in the Nagumo equation literature and their existence verification is relatively straightforward. The existence of pulse solutions, however, is more difficult. We have related existence to the pulse’s relation to the “unstable root” of the reaction term, i.e., $\phi = a$, pointwise. At any point along the solution the solution is either above, below, or crossing a . The series of lemmas and theorems presented supply conditions, based on the derived candidate solutions, for verifying that these conditions are true, i.e., that a one-pulse solution crosses a exactly twice. Among the items that our numerical investigations of the solution behavior illustrate are

- that for single fronts more than one solution can exist;
- that for single pulses there is a range of a values such that there exists at least two distinct pairs of solution pulses;
- that the speed of front solutions can be seen as a bound for the speed of pulse solutions;
- that the distance between multiple pulse shows a dependence on the parameter a ;
- that the spatially discrete diffusion operator retards propagation when compared to the spatially continuous diffusion operator.

Acknowledgments. The authors are grateful to Chris Lee and Paul Raff, who helped initiate this investigation as part of the REU site program DMS-9912293 at Colorado School of Mines.

REFERENCES

- [1] A. R. A. ANDERSON AND B. D. SLEEMAN, *Wave front propagation and its failure in coupled systems of discrete bistable cells modelled by FitzHugh-Nagumo dynamics*, Internat. J. Bifur. Chaos Appl. Sci. Engrg., 5 (1995), pp. 63–74.
- [2] C. G. ARONSON AND H. F. WEINBERGER, *Multidimensional nonlinear diffusion arising from population genetics*, Adv. Math., 30 (1978), pp. 33–76.
- [3] P. W. BATES, X. CHEN, AND A. J. J. CHMAJ, *Traveling waves of bistable dynamics on a lattice*, SIAM J. Math. Anal., 35 (2003), pp. 520–546.
- [4] J. BELL AND C. COSNER, *Threshold behavior and propagation for nonlinear differential-difference systems motivated by modeling myelinated axons*, Quart. Appl. Math., 42 (1984), pp. 1–114.
- [5] S. N. CHOW, J. MALLET-PARET, AND W. SHEN, *Traveling waves in lattice dynamical systems*, J. Differential Equations, 149 (1998), pp. 248–291.
- [6] J. W. CAHN, *Theory of crystal growth and interface motion in crystalline materials*, Acta Met., 6 (1960), pp. 554–561.
- [7] J. W. CAHN, J. MALLET-PARET, AND E. S. VAN VLECK, *Traveling wave solutions for systems of ODEs on a two-dimensional spatial lattice*, SIAM J. Appl. Math., 59 (1998), pp. 455–493.
- [8] A. CARPIO AND L. L. BONILLA, *Pulse propagation in discrete systems of coupled excitable cells*, SIAM J. Appl. Math., 63 (2002), pp. 619–635.
- [9] S. BINCZAK, J. C. EILBECK, AND A. C. SCOTT, *Ephaptic coupling of myelinated nerve fibers*, Phys. D, 148 (2001), pp. 159–174.
- [10] B. DENG, *The existence of infinitely many traveling front and back waves in the FitzHugh–Nagumo equations*, SIAM J. Math. Anal., 22 (1991), pp. 1631–1650.
- [11] C. E. ELMER, *Multiple Planar Interfaces for Crystalline Materials with Spatially Discrete Gradient Energy*, preprint, 2005.
- [12] C. E. ELMER AND E. S. VAN VLECK, *Analysis and computation of traveling wave solutions of bistable differential-difference equations*, Nonlinearity, 12 (1999), pp. 771–798.
- [13] C. E. ELMER AND E. S. VAN VLECK, *Traveling wave solutions for bistable differential-difference equations with periodic diffusion*, SIAM J. Appl. Math., 61 (2001), pp. 1648–1679.
- [14] T. ERNEUX AND G. NICOLIS, *Propagating waves in discrete bistable reaction-diffusion systems*, Phys. D, 67 (1993), pp. 237–244.
- [15] J. EVANS, *Nerve axon equations I: Linear approximations*, Indiana Univ. Math. J., 21 (1972), pp. 877–955.
- [16] J. EVANS, *Nerve axon equations II: Stability at rest*, Indiana Univ. Math. J., 22 (1972), pp. 75–90.
- [17] J. EVANS, *Nerve axon equations III: Stability of the nerve impulse*, Indiana Univ. Math. J., 22 (1972), pp. 577–594.
- [18] J. EVANS, *Nerve axon equations IV: The stable and unstable impulse*, Indiana Univ. Math. J., 24 (1975), pp. 1169–1190.
- [19] G. FATH, *Propagation failure of traveling waves in discrete bistable medium*, Phys. D, 116 (1998), pp. 176–190.
- [20] J. A. FEROE, *Existence and stability of multiple impulse solutions of a nerve equation*, SIAM J. Appl. Math., 42 (1982), pp. 235–246.
- [21] P. C. FIFE AND J. B. MCLEOD, *The approach of solutions of nonlinear diffusion equations to travelling front solutions*, Arch. Ration. Mech. Anal., 65 (1977), pp. 335–361.
- [22] R. FITZHUGH, *Impulses and physiological states in theoretical models of nerve membrane*, Biophys. J., 1 (1961), pp. 445–466.
- [23] W.-Z. GAO, *Threshold behavior and propagation for a differential-difference system*, SIAM J. Math. Anal., 24 (1993), pp. 89–115.
- [24] S. HEINZE, G. PAPANICOLAOU, AND A. STEVENS, *Variational principles for propagation speeds in inhomogeneous media*, SIAM J. Appl. Math., 62 (2001), pp. 129–148.
- [25] C. K. R. T. JONES, *Stability of the traveling wave solution of the FitzHugh-Nagumo system*, Trans. Amer. Math. Soc., 286 (1984), pp. 431–469.
- [26] J. P. KEENER, *Propagation and its failure in coupled systems of discrete excitable cells*, SIAM J. Appl. Math., 47 (1987), pp. 556–572.
- [27] J. P. KEENER, *The effects of discrete gap junction coupling on propagation in myocardium*, J. Theoret. Biol., 148 (1991), pp. 49–82.

- [28] J. KEENER AND J. SNEYD, *Mathematical Physiology*, Springer-Verlag, New York, 1998.
- [29] M. KRUPA, B. SANDSTEDTE, AND P. SZMOLYAN, *Fast and slow waves in the FitzHugh-Nagumo equation*, J. Differential Equations, 133 (1997), pp. 49–97.
- [30] K. MAGINU, *Geometrical characteristics associated with stability and bifurcations of periodic travelling waves in reaction-diffusion systems*, SIAM J. Appl. Math., 45 (1985), pp. 750–774.
- [31] J. MALLET-PARET, *The Fredholm alternative for functional differential equations of mixed type*, J. Dynam. Differential Equations, 11 (1999), pp. 1–48.
- [32] J. MALLET-PARET, *The global structure of traveling waves in spatially discrete dynamical systems*, J. Dynam. Differential Equations, 11 (1999), pp. 49–128.
- [33] H. MCKEAN, *Nagumo's equation*, Adv. Math., 4 (1970), pp. 209–223.
- [34] J. NAGUMO, S. ARIMOTO, AND S. YOSHIZAWA, *An active pulse transmission line simulating nerve axon*, Proc. Inst. Radio Engrg., 50 (1964), pp. 2061–2070.
- [35] J. RINZEL AND J. B. KELLER, *Traveling wave solutions of a nerve conduction equation*, Biophys. J., 13 (1973), pp. 1313–1337.
- [36] A. SCOTT, *Neuroscience, A Mathematical Primer*, Springer-Verlag, New York, 2002.
- [37] L. F. SHAMPINE, R. C. ALLEN, AND S. PRUESS, *Fundamentals of Numerical Computing*, Wiley, New York, 1997.
- [38] A. TONNELIER, *Wave propagation in discrete media*, J. Math. Biol., (2001), pp. 1–19.
- [39] A. TONNELIER, *The McKean's caricature of the FitzHugh-Nagumo model I. The space-clamped system*, SIAM J. Appl. Math., 63 (2002), pp. 459–484.
- [40] A. TONNELIER, *The McKean's caricature of the FitzHugh-Nagumo model: Traveling pulses in discrete diffusive medium*, Phys. Rev. E (3), 67 (2003), 036105.
- [41] W.-P. WANG, *Multiple impulse solutions to McKean's caricature of the nerve equation. I. Existence*, Comm. Pure Appl. Math., 41 (1988), pp. 71–103.
- [42] W.-P. WANG, *Multiple impulse solutions to McKean's caricature of the nerve equation. II. Stability*, Comm. Pure Appl. Math., 41 (1988), pp. 997–1025.
- [43] E. YANAGIDA, *Stability of fast travelling pulse solutions of the FitzHugh-Nagumo equation*, J. Math. Biol., 22 (1985), pp. 81–104.
- [44] B. ZINNER, *Stability of traveling wavefronts for the discrete Nagumo equation*, SIAM J. Math. Anal., 22 (1991), pp. 1016–1020.
- [45] B. ZINNER, *Existence of traveling wavefront solutions for the discrete Nagumo equation*, J. Differential Equations, 96 (1992), pp. 1–27.